WILEY | Hindawi

Research Article

Thermal Performance and Technoeconomic Analysis of Solar-Assisted Heat Pump Dryer Integrated with Energy Storage Materials for Drying Cavendish Banana (*Musa acuminata*)

Aldé Belgard Tchicaya Loemba [ID],[1] **Baraka Kichonge** [ID],[1,2] **and Thomas Kivevele** [ID][1]

[1]*School of Materials, Energy, Water and Environmental Sciences (MEWES), The Nelson Mandela African Institution of Science and Technology (NM-AIST), P.O. Box 447, Arusha, Tanzania*
[2]*Mechanical Engineering Department, Arusha Technical College, P.O. Box 296, Arusha, Tanzania*

Correspondence should be addressed to Thomas Kivevele; thomas.kivevele@nm-aist.ac.tz

This study examines a novel solar-assisted heat pump dryer integrated with a thermal energy storage system using soapstone as storage material. The dryer is investigated through experimental analysis across three operating modes: mode 1 with thermal energy storage during daytime, mode 2 without thermal energy storage during nighttime, and mode 3 without thermal energy storage during daytime. Experiments were carried out to investigate the drying of 500 g of Cavendish banana. Thermal performance, as well as economic, and nutritional content were examined. Three replicates of the experiment yielded consistent results, showing a significant reduction in the moisture content of the initial sample from 74.4% to 9.6% after undergoing distinct drying durations. Mode 1 achieved this reduction in 270 minutes, mode 2 in 390 minutes, and mode 3 in 360 minutes. The average specific moisture extraction rates for modes 1, 2, and 3 were 0.13, 0.11, and 0.12 kg/kWh, respectively. Simultaneously, the drying rate ranged from 0.16 to 0.24% per minute. The drying efficiency varied among the tested modes, with mode 1 achieving the highest efficiency at 23.23%. In terms of coefficient of performance, mode 1, mode 2, and mode 3 exhibited values of 3.69, 2.57, and 2.54, respectively. The economic analysis conducted specifically for mode 1 revealed a payback period of 1.5 years, indicating the time required to recover the initial investment. Additionally, the results indicated that the dried Cavendish banana had significantly higher concentrations of proximate parameters and minerals compared to the fresh Cavendish banana, as evidenced by a p value less than 0.05.

1. Introduction

Agricultural products are generally very sensitive to temperature. The drying of these products therefore requires the use of adequate drying techniques or methods to retain most of the nutrients that the product possesses when subjected to the drying operations. Open sun drying, for example, which is one of the commonly adopted drying methods in most rural areas of Africa, has proven to be ineffective in retaining the nutritional properties of dried products [1]. To preserve the nutritional properties of dried products, new methods such as fluidized bed drying, freeze-drying, spouted bed drying, air-drying, and vacuum drying have been developed [2].

Despite the fact that these dryers have been successful in enhancing the quality of dried products by meeting consumer demands for the preservation of nutritious properties, they do have some downsides, such as the high energy consumption. The development of heat pump dryers has been one of the options to deal with drawbacks observed in some of the developed dryers [3]. Heat pump dryers are characterized with low energy consumption, high coefficient of performance, high drying efficiency, controllable temperature, low drying times, and less loss of quality of the dried products. Heat pump dryer can operate over a wide temperature and humidity range, providing the optimum conditions for drying heat-sensitive agricultural products [4].

To optimize the efficiency of heat pump dryers, many researchers are employing solar energy as an additional heat source for heat pump dryers because it is one of the most commonly accessible natural energies and renewable sources. As a result, incorporating solar energy into heat pump dryers is regarded as a realistic option [5, 6]. Around the world, many studies have been reported on the combined use of heat pump dryers and solar energy for drying agricultural products in order to optimize their drying and thermal performances; the system is named as solar-assisted heat pump dryer (SAHPD) [7, 8]. For drying coriander, Alishah et al. [9] developed a SAHPD. According to the findings, this technology significantly reduced the drying time down to 25% and energy consumption down to 12% and increased the coefficient of performance up to 2.32 and the specific moisture extraction rate up to 20%. Prasanna and Manjula [10] came to the same conclusions after reviewing the design and the performance of SAHPD systems used for drying agricultural products. The study demonstrated that SAHPDs use little energy and are more thermally efficient. Furthermore, compared to products dried using, for instance, conventional hot air dryers, the products dried using solar-assisted heat pump dryer systems had greater color and aroma properties. To dry banana chips, Singh et al. built a solar heat pump dryer with infrared assistance. Four operational modes were used to test the performance of the proposed dryer: solar-infrared-assisted heat pump drying mode, solar-assisted heat pump drying mode, infrared-assisted heat pump drying mode, and heat pump drying mode. The findings demonstrate that the greatest specific moisture extraction rate was achieved by the solar-assisted heat pump drying [11]. The same authors have also conducted another study comparing the performance of a heat pump dryer alone and a solar-assisted heat pump dryer to dry banana chips at a constant air flow rate. The results show that the solar-assisted heat pump dryer has higher energy and exergy efficiencies [12].

The interest in solar-assisted heat pump dryers is growing worldwide, driven by advancements in their design and manufacturing. However, there is still room for improvement, especially in utilizing these dryers effectively during cloudy periods with intermittent solar energy. Researchers propose hybrid SAHPDs that incorporate various options such as solar, coulomb force, radiofrequency, biomass, ultrasonic, or waste heat recovery. Unfortunately, there are limited studies on integrating thermal storage systems to enhance SAHPD performance. Additionally, no study has explored the use of natural rocks as energy storage materials in integrated SAHPDs. Combining SAHPDs with thermal energy storage using natural rocks shows promise for maximizing efficiency [4, 13–15]. Moreover, there are limited research on the economic analysis of SAHPDs, making it challenging to have a comprehensive understanding of the economic consequences or benefits of SAHPD integrated with energy storage system. Singh et al. [16] investigated the economic analysis of SAHPD and found that initial costs were higher while operational costs were lower. When drying rice with a SAHPD combined with a biomass furnace, Yahya et al. obtained a payback period of 1.6 years (M.

[8]). In addition, the attention given to Cavendish banana (*Musa acuminata*) in the existing literature has been relatively limited, as indicated by the findings in Table 1. Sub-Saharan Africa, in particular, lacks familiarity with solar-assisted heat pump dryers (SAHPDs), and there is a notable absence of research on utilizing SAHPDs for drying Cavendish banana under the specific climatic conditions of Tanzania [4]. As a result, the primary objective of this study is to address this research gap by investigating a novel SAHPD that incorporates a thermal energy storage system utilizing soapstone as the storage material. In this study, the dryer is tested for drying Cavendish banana (*Musa acuminata*). The evaluation of thermal performance will encompass several crucial parameters, including the analysis of moisture content, drying rate, specific moisture extraction rate, coefficient of performance, and drying efficiency. These factors play a significant role in determining the effectiveness of the drying process and the overall performance of the SAHPD system. Furthermore, this research aims to provide a comprehensive analysis of the economic feasibility of implementing the proposed SAHPD system. It will examine important economic indicators such as capital costs, operating costs, approximate profitability measures, and rigorous profitability measurements. These evaluations will shed light on the economic viability and potential returns on investment associated with deploying the SAHPD system for drying Cavendish banana.

In addition to the thermal and economic aspects, the study will delve into the proximate and mineral analyses of both fresh and dried Cavendish bananas. Vitamin C and B6 are also examined in this study. These analyses will provide insights into the changes in nutrient composition that occur during the drying process. By assessing the nutritional changes in Cavendish banana resulting from the drying process, the study will contribute valuable information regarding the impact of the proposed SAHPD system on the overall nutritional quality of the dried product. Overall, this study is aimed at filling the knowledge gap surrounding the drying of Cavendish banana using SAHPDs in the specific climatic conditions of Tanzania. It seeks to provide a thorough understanding of the thermal performance, economic viability, and nutritional implications associated with the proposed SAHPD system. By conducting a comprehensive investigation, this research is aimed at contributing to the advancement of drying technologies for Cavendish banana and potentially paving the way for its commercial application in Tanzania and other regions with similar climatic conditions.

2. Materials and Methods

2.1. Basic Design Calculation. The amount of moisture to be removed from the Cavendish banana (*Musa acuminata*) during the drying process was calculated using [23–26]

$$M = \frac{W(M_i - M_f)}{100 - M_f}. \tag{1}$$

TABLE 1: Summary of experimental results obtained by references when drying Cavendish banana.

Drying mode	Mass	Thickness	Drying temperature	Drying time	Initial moisture content	Final moisture content	Drying rate
Convective hot air-drying [17]	NA	3 mm	35, 40, 45, and 50°C	For 35°C, 40°C, 45°C, and 50°C, the drying times ranged from 1320 to 1440 minutes, 1140 to 1440 minutes, 840 to 1020 minutes, and 660 to 840 minutes, respectively.	3.039, 3.023, 3.535, and 3.255 kg/kg dry solid, respectively, for 35, 40, 45, and 50°C.	0.21, 0.199, 0.24, and 0.214 kg/kg dry solid, respectively, for 35, 40, 45, and 50°C.	NA
Fixed-bed tray dryer [18]	NA	Bananas were cut longitudinally and transversally, resulting in 4 pieces.	65°C	1440 minutes	76%	19.32%	NA
Convection oven [19]	NA	5 mm	50, 60, and 70°C	360, 210, and 180 minutes, respectively for 50, 60, and 70°C.	76.65%	Up to steady state (value not available)	NA
Radio frequency vacuum dryer [20]	NA	8 mm	52°C (maximum)	270 minutes	3.34–3.67 g/g (dry basis)	0.7 g/g (dry basis)	NA
Solar dryer dome [21]	NA	Bananas were not sliced.	40, 50, 60, 70, and 80°C	9600 to 9960 minutes	78.25%	26%	NA
Heat pump dehumidifier dryer [22]	5 kg	Bananas were not sliced.	50°C	2484 minutes	269% (dry basis)	25% (dry basis)	0.060

M_i is the initial moisture content; M_f is the estimated final moisture content; W is the mass of banana to be dried.

The energy required to remove the moisture content was calculated using [23, 26, 27]

$$E\,(\text{kJ}) = WC_{\text{pm}}(T_2 - T_1) + I_V M. \quad (2)$$

W is the mass of the product to be dried (kg); C_{pm} is the specific heat of the product; M is the amount of moisture to be removed (kg), T_2 is the estimated temperature of drying air; T_1 is the ambient air; I_v is the latent heat of vaporization of water [27]. Therefore, the energy required per hour can be obtained using [23]

$$Q(kJ) = \frac{E(\text{kJ})}{\text{Drying time}}. \quad (3)$$

The heat pump used in this system must have the capacity to supply this energy required per hour (Q).

The collector area was calculated using [24]

$$A_C = \frac{Q}{I \times \eta}, \quad (4)$$

where Q (kJ) is the energy required to remove the moisture content; I (kJ/m^2) is the total radiation on the horizontal surface during the drying period, and η is the collector efficiency.

By considering that the amount of energy stored in the storage system is equal to the energy supply by the solar collector, the volume of the storage energy system (V) was calculated using [28]

$$Q = \rho V C_P(T_2 - T_1). \quad (5)$$

The area of the drying chamber (A_d) was estimated using [23]

$$A_d = \frac{V_b}{E_b}, \quad (6)$$

with

$$V_b = \frac{M_b}{\rho_b}. \quad (7)$$

V_b is the bulk volume; E_p is the thickness of banana; M_b is the mass of Cavendish banana, and ρ_b is the bulk density.

2.2. Experimental Setup.

The experimental setup was established at Arusha Technical College (ATC) in Tanzania, in accordance with the methodology described in the authors' previous publication [13]. Arusha, located in a temperate climate region on the eastern side of the Great Rift Valley, below Mount Meru, was selected as the site for the study. A 3D diagram, presented in Figure 1, depicts the configuration of the solar-assisted heat pump dryer (SAHPD) inte-

grated with a thermal energy storage (TES) system. The main components of this integrated system comprise the drying chamber, the heat pump system, the solar collector, and the thermal energy storage system that employs soapstone as the storage medium. The thermal energy storage system efficiently captures and stores solar energy in the soapstone medium through the mechanism of sensible heat. The stored energy is subsequently utilized to preheat the air entering the storage system before it reaches the heat pump's condenser. In summary, the decision to incorporate soapstone as the storage material in the system is aimed at achieving energy optimization and overall efficiency improvements. By capitalizing on the advantageous thermal properties of soapstone, the system can effectively store and utilize solar energy, resulting in enhanced energy efficiency and improved performance during the drying process. Before assembling, each component of the dryer was built step-by-step and independently. 1.5 mm galvanized steel sheets were used to construct the inner and outer parts of the drying chamber, which has an area of 3.6 m^2. Fiberglass, a commonly used thermal insulation material [29], with a thickness of 6 mm, was used to fill the gap between the inner and outer parts of the drying chamber to prevent the heat inside the drying chamber from escaping. The outer part of the drying chamber was covered with sheets of 1.5 mm thick galvanized steel sheets. In the upper part of the drying chamber, a 70 cm solar chimney constructed of a 1.5 mm thick mild steel sheet with a roof turbine ventilator at one end has also been installed. The roof turbine ventilator made of stainless steel has a thickness of 300 mm. It applies the theory of convection between natural wind and air to accelerate and transform any parallel airflow into vertical so as to improve the indoor ventilation and effectively remove indoor soot, odor, moisture, dust, etc. Eight trays were placed in the drying chamber. The trays were made with plastic wire mesh to allow hot air from the drying chamber condenser to circulate. Mild steel sheets were used to create the drying chamber frame assembly. The heat pump system consists of four basic components: a 4-horsepower evaporator, a 4-horsepower condenser, a 4-horsepower compressor, and an expansion valve (3/8 × 1/2 inches). R-22, also known as R22 freon and HCFC-22 freon, was used as a refrigerant in the heat pump system.

The solar collector and the thermal energy storage system have been constructed as a single system. The solar collector has been placed at the top, and the thermal energy storage has been placed at the bottom. The solar collector was made with a glass 6 cm thick, 1 m long, and 70 cm wide. An aluminum sheet painted black and 0.5 mm thick has been positioned at the bottom of the glass to allow the best capture of solar radiation. The storage unit was the same length and width as the glass placed above the solar collector. To limit heat loss, a layer of insulating materials with a thickness of 8 cm was placed between the inner and outer parts of the storage unit. Three different tube exchangers made from aluminum sheets and using a counterflow configuration were placed in parallel inside the storage unit. The counterflow configuration was used to help maximize
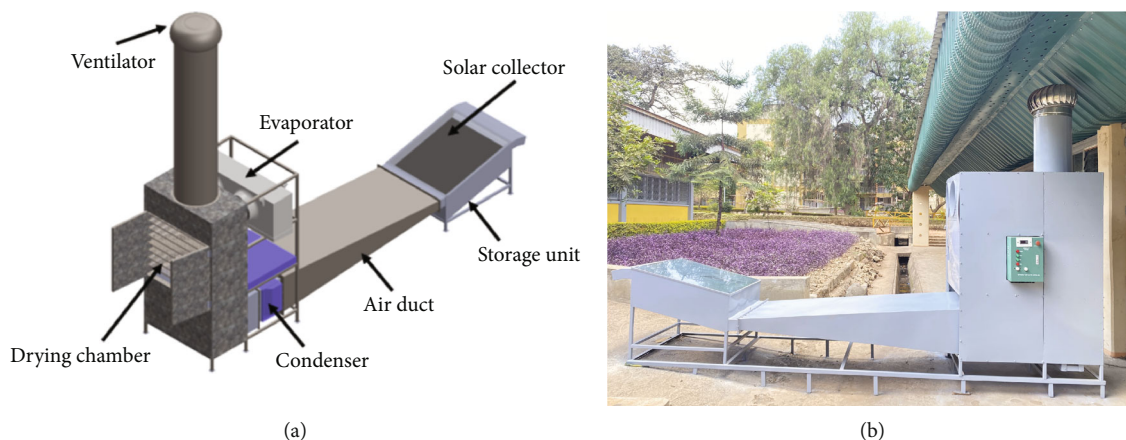
(a)

(b)

FIGURE 1: 3D diagram (a) and photo (b) of the solar-assisted heat pump dryer integrated with thermal energy storage [13].

TABLE 2: Measurement instruments and uncertainty.

Instruments	Parameters	Range	Accuracy	Resolution	Error (%)
Anemometer	Air velocity	0 to 30 m/s	±5%	0.1 m/s	0.141421
Temperature humidity data logger (SSN-22)	Temperature and humidity	Temperature: -35 to 80	Temperature: ±3 °C	±0.1 °C	0.2
		Humidity: 0 to 100%	Humidity: ±3%	0.1 RH	0.2
Thermocouple temperature data logger (SSN-61)	Temperature	-180 to 1250 °C	±5%	±0.1 °C	0.2
Digital balance (FF1976)	Weight	2 to 400 g	5 g/10 g	0.1 g	0.141421
Solar power meter	Irradiance	2000 W/m^2	±5%	0.1 W/m^2	0.141421
Temperature sensor	Temperature and humidity	Temperature: -40 to 80 °C	Temperature: ±0.5 °C	±0.1 °C	0.2
		Humidity: 0 to 100%	Humidity: 2-5%	0.01 RH	0.2
CT sensor	Power consumption	10 mA to 100 A	±3%	0.1	0.141421

the heat transfer between the cold air entering the storage unit and the soapstone placed inside the exchanger tubes. The storage material used in the storage unit was soapstone. After being collected from Ngaka hill, which is located in the village of Kikombo-Mnadani, in the urban district of Dodoma in Tanzania, this storage material was cut into cubes having edges measuring 2 cm each, and then, they were placed not inside the exchanger tubes but in all the storage spaces left empty by the three exchanger tubes.

2.3. *Experimental Procedure.* All experiments were conducted at Arusha Technical College (ATC), located in the city of Arusha, Tanzania, using SAHPD with TES shown in Figure 1. In this study, the Cavendish banana fruit, known for its nutritional benefits and commonly referred to as Kimalindi in Tanzania, was purchased from the Kilombero market, a local market that is one of the largest marketplaces in the city of Arusha. Once purchased, the Cavendish banana fruit was carefully cleaned in water, peeled, and then cut into slices ranging in thickness from 1 to 2 mm before being put on the trays placed in the drying chamber. The mass of Cavendish banana was 500 g. For each mode of operation, the experiment was repeated for three days to

get a respectable average as proposed by Singer et al. [30]. The initial moisture content of banana was determined using a common method of drying a sample in an oven and calculating moisture content by the weight difference between dry and wet material. The initial moisture content of banana was found to be 74.4% wet basis (w.b). To carry out these experiments, three operating modes of the developed dryer were used, i.e., SAHPD with TES during daytime (mode 1), SAHPD without TES during nighttime (mode 2), and the SAHPD without TES during daytime (mode 3). All of these experiments were conducted for the sole purpose of analyzing the economic consequences and evaluating the performance of the dryer developed under different operating modes. Furthermore, the proximate analysis and the mineral and vitamin analyses of fresh and dried Cavendish banana fruit were performed.

2.4. *Data Measurements and Uncertainty Analysis.* Details about the measured parameters, the instruments utilized for data collection, and their specific characteristics are outlined in Table 2. Data was collected both manually and automatically at 30-minute intervals. The uncertainties will be evaluated using [31]

$$U_R = \sqrt{\left[\left(\frac{\partial R}{\partial x_1} U_1\right)^2 + \left(\frac{\partial R}{\partial x_2} U_2\right)^2 + \left(\frac{\partial R}{\partial x_3} U_3\right)^2 + \cdots \left(\frac{\partial R}{\partial x_n} U_n\right)^2\right]}. \tag{8}$$

The total uncertainty for the measurement of temperatures at various places such as the inlet of the drying chamber (U_{TI}), outlet of the drying chamber (U_{TO}), and ambient temperature (U_{TA}) and readings ($U_{Reading}$) is calculated using

$$
\begin{aligned}
U_{Temperature} &= \sqrt{U_{Measurement}^2 + U_{Reading}^2} \\
&= \sqrt{U_{TI}^2 + U_{TO}^2 + U_{TA}^2 + U_{Reading}^2} \\
&= \sqrt{(0.1)^2 + (0.1)^2 + (0.1)^2 + (0.1)^2} = 0.2\%.
\end{aligned}
\tag{9}
$$

The total uncertainty for the measurement of relative humidity at various places such as the inlet of the drying chamber (U_{RHI}), outlet of the drying chamber (U_{RHO}), and ambient temperature (U_{RHA}) and readings ($U_{Reading}$) is calculated using

$$
\begin{aligned}
U_{Humidity} &= \sqrt{U_{Measurement}^2 + U_{Reading}^2} \\
&= \sqrt{U_{RHI}^2 + U_{RHO}^2 + U_{RHA}^2 + U_{Reading}^2} \\
&= \sqrt{(0.1)^2 + (0.1)^2 + (0.1)^2 + (0.1)^2} = 0.2\%.
\end{aligned}
\tag{10}
$$

The total uncertainty for the measurement of weight loss is calculated using

$$
\begin{aligned}
U_{Weight} &= \sqrt{U_{Measurement}^2 + U_{Reading}^2} \\
&= \sqrt{(0.1)^2 + (0.1)^2} = 0.141421\%.
\end{aligned}
\tag{11}
$$

The total uncertainty for the measurement of solar radiation is calculated using

$$
\begin{aligned}
U_{Radiation} &= \sqrt{U_{Measurement}^2 + U_{Reading}^2} \\
&= \sqrt{(0.1)^2 + (0.1)^2} = 0.141421\%.
\end{aligned}
\tag{12}
$$

The total uncertainty for the measurement of power consumption is calculated using

$$
\begin{aligned}
U_{Power} &= \sqrt{U_{Measurement}^2 + U_{Reading}^2} \\
&= \sqrt{(0.1)^2 + (0.1)^2} = 0.141421\%.
\end{aligned}
\tag{13}
$$

The total uncertainty for the measurement of wind is calculated using

$$
\begin{aligned}
U_{wind} &= \sqrt{U_{Measurement}^2 + U_{Reading}^2} \\
&= \sqrt{(0.1)^2 + (0.1)^2} = 0.141421\%.
\end{aligned}
\tag{14}
$$

Then, the total uncertainty of the drying experiment may be calculated using

$$
\begin{aligned}
U_{total} &= \sqrt{U_{Temperature}^2 + U_{humidity}^2 + U_{Weight}^2 + U_{Radiation}^2 + U_{Power}^2 + U_{wind}^2} \\
&= 0.982693\%.
\end{aligned}
\tag{15}
$$

2.5. Performance Analysis

2.5.1. Moisture Content and Drying Rate. The moisture content and drying rate were calculated, respectively using [32, 33]

$$
\begin{aligned}
MC_{wb} &= \frac{MC_i - MC_f}{MC_i} \times 100, \\
DR &= \frac{MC_{t+dt} - MC_t}{dt}.
\end{aligned}
\tag{16}
$$

2.5.2. Condenser Heating Capacity. Equation (17) was used to determine how much heat a condenser rejects:

$$Q_{cond} = \dot{m}_a C_{P,a} (T_{amb} - T_{cond}), \tag{17}$$

with

$$
\begin{aligned}
\dot{m}_a &= \rho_a * S * v, \\
\rho_a &= 1.292 \frac{273.15}{Ta(K)}, \\
C_{P,a} &= 1.0029 + 5.410^{-5} T_a.
\end{aligned}
\tag{18}
$$

Q_{cond} is the condenser heating capacity (kW), $\dot{m}_a$ is the mass flow rate of the air (kg/s), S is the surface of the drying chamber, v is the velocity of air in the drying chamber, ρ_a is the air density in the drying chamber, $C_{P,a}$ is the specific heat of air (kJ/kg°C), T_{amb} is the ambient temperature (°C), and T_{cond} is the air temperature at the outlet of the condenser (°C) [34].

2.5.3. Coefficient of Performance. When using the heat pump mode alone, the coefficient of performance (COP) was determined by dividing the quantity of heat delivered by the condenser by the total energy consumed by the whole system as shown in [34]

$$COP_{HP} = \frac{Q_{cond}}{Q_{total\,consumed}}. \tag{19}$$

Q_{cond} is the condenser heating capacity calculated using equation (10), and $Q_{total\,consumed}$ is the total energy consumed by the whole system obtained using a CT sensor.

2.5.4. Specific Moisture Extraction Rate.

The specific moisture extraction rate (SMER) will be calculated using [33, 35]

$$\text{SMER} = \frac{M_w}{\text{Total energy input per unit time}}. \quad (20)$$

SMER is the specific moisture extraction rate (kg/kWh), and M_w is the mass of water removed (kg).

Where:

$$M_w = \frac{M_p(\text{MC}_i - \text{MC}_f)}{(100 - \text{MC}_f)}. \quad (21)$$

MC_f is the final moisture content of the product (kg), M_p is the mass of fresh samples, and MC_i is the initial moisture content of the product (kg).

2.5.5. Efficiency of the Solar Collector Integrated with Soapstone.

The efficiency of solar collector integrated with soapstone as storage material was evaluated using [36]

$$\eta_{\text{col}} = \frac{E_{\text{stored}}}{E_{\text{stored,max}}} \times 100. \quad (22)$$

$E_{\text{stored}} = mC_P(T_{\text{out,col}} - T_{\text{in,col}})$ is the energy stored at time t, and $E_{\text{stored,max}}$ is the maximum energy stored at time t.

2.5.6. Dryer Efficiency.

The drying efficiency is calculated using

$$\eta_d = \frac{L_v M_w}{Q_{\text{total consumed}}} \times 100. \quad (23)$$

L_V is the latent heat of vaporization of water, M_w is the mass of water removed (kg), and $Q_{\text{total consumed}}$ is the total energy consumed by the whole dryer (kWh).

2.6. Proximate Analysis

2.6.1. Preparation of Sample.

The fresh and dried Cavendish banana (*Musa acuminata*) were ground into fine powder form, using an electric blender. The fine powder was then used in the analysis.

2.6.2. Analysis of Sample.

Proximate analysis was carried out on the powdered Cavendish banana (*Musa acuminata*), to determine the presence of moisture, protein, fat, ash, crude fiber, and carbohydrate by using standard analytical methods as described by the Official Methods of Association of Official Analytical Chemists (OAOC) [37, 38].

2.6.3. Determination of Moisture Content.

Moisture content was determined by the oven drying method. Five grams of powdered sample was accurately weighed and placed in a clean and dry Petri dish. The sample was dried in an oven at 105°C for 24 hours until a constant weight was obtained. Then, the sample was placed in the desiccator for 30 minutes to cool. After cooling, it was weighed again, taking care not to expose the sample to the atmosphere. The moisture content (%) was calculated using [37]

$$\text{MC}(\%) = \frac{\text{Moisture weight}}{\text{Weight of sample(g)}} \times 100. \quad (24)$$

2.6.4. Determination of Ash Content.

A dry ashing method was used to determine ash contents. A clean empty crucible was placed in a muffle furnace at 550°C or an hour to ensure that all possible impurities on the surface of crucible were burned off and then cooled in a desiccator for 30 minutes, and then, the weight of the empty crucible was noted. Five grams of sample was placed in the crucible. The crucible with its content was placed in a muffle furnace and heated for 24 hours. After complete heating, the sample in crucible was cooled down in the desiccator. The ash content (%) was calculated using [37]

$$\text{Ash content}(\%) = \frac{\text{Weight of ash(g)}}{\text{weight of sample(g)}} \times 100. \quad (25)$$

2.6.5. Determination of Crude Protein.

The crude protein was determined by the Kjeldahl method, as described in the Association of Official Analytical Chemists (AOAC) [37]. According to this method, samples were digested by heating with concentrated sulphuric acid (H_2SO_4) in the presence of Kjeldahl catalyst. The mixture was then made alkaline and distilled into a boric acid solution. The borate ions formed were titrated against standard sulphuric acid 0.05 N, which is converted to total nitrogen in the sample, then multiplied by a 6.25 conversion factor to crude protein.

$$\text{Nitrogen}(\%) = \frac{(Vs - Vb) \times N \times 1.401}{\text{weight of sample(g)}} \times 100,$$

$$\text{CP}(\%) = \text{Nitrogen}(\%) \times 6.25. \quad (26)$$

2.6.6. Determination of Fat Content.

Total fat was determined by using the Soxhlet ether extraction in which five grams of powdered sample was placed into the extraction thimble and assembled to the Soxhlet apparatus. The petroleum ether 70 ml was used for the extraction process in three automatic phases in a fat analyzer machine. The boiling phase was conducted for 15 minutes, the rinsing phase for 30 minutes, and the petroleum ether recovery phase for 10 minutes. The remaining petroleum ether was then evaporated in the oven. Preweighed cups containing fat were dried in an oven at 105°C for 1 hour to evaporate any remaining petroleum ether and then cooled in a desiccator for 30 minutes and reweighed. Percentage fat was calculated by using [37]

$$\text{Fat content}(\%) = \frac{\text{Weight of crude fat(g)}}{\text{Weight of sample(g)}}. \quad (27)$$

2.6.7. Determination of Crude Fiber.

This analysis involves two stages of digestion which were acid and alkaline solution, using the method described by the Association of

Official Analytical Chemists (AOAC) [37], and the crude fiber is calculated; thus

$$\text{Crude fiber}(\%) = \frac{(\text{Weight of residual} - \text{Weight of ash})}{\text{Weight of sample}(\text{g})} \times 100. \tag{28}$$

2.6.8. Determination of Total Carbohydrate. Total soluble carbohydrate was determined by the difference of the sum of all the proximate composition from 100% [38].

2.6.9. Determination of Energy. The nutritional energy value (calorie) was determined by multiplying the number of grams of carbohydrate, protein, and fat by 4, 4, and 9, respectively.

2.7. Mineral and Vitamin Analyses

2.7.1. Minerals. The minerals, which include copper, iron, phosphorus, calcium, zinc, and manganese, were identified by incinerating one gram of the homogenized sample for four hours at 450°C in a furnace. The ashes from the sample were then mixed with 10 ml of a 6% hydrochloric acid solution, filtered through Whatman filter papers, and then diluted with 100 ml of distilled water. Afterwards, an atomic absorption spectrophotometer was used to read the filtrates [39].

2.7.2. Vitamin C. Five grams of homogenized sample was used for the determination of vitamin C, and 25 milliliters of 10% trichloroacetic acid was added after the homogenized sample was ground in a mortar and pestle. The extracted sample was then put into a 50 ml volumetric flask and diluted with trichloroacetic acid solution to the appropriate concentration. Afterwards, Whatman filter papers were used to filter the diluted sample. After that, the filtrates were read using a UV/Vis spectrophotometer [40].

2.7.3. Vitamin B6. One gram of the material was homogenized with 50 ml of 0.1 N HCL (hydrochloric acid), transferred to a 125 ml Erlenmeyer flask, filtered, and degassed for five minutes to determine vitamin B6. A degassed sample of 10 ml was placed in volumetric flasks, which were subsequently diluted with 0.1 N HCL, and absorbance was determined [41].

2.8. Statistical Analysis. The one-way analysis of variance (ANOVA) was used in Microsoft Excel to statistically assess the proximate, minerals, and vitamin data.

2.9. Economic Analysis. The key economic indicators analyzed were the CapEX (capital costs), the OpEX (operating costs), the approximate profitability measures, and the rigorous profitability measures.

2.9.1. CapEX. CapEX was calculated by adding the costs of all components or equipment and the labor costs during the manufacturing:

$$\text{CapEX} = C_E + C_L. \tag{29}$$

C_E and C_L are, respectively, the equipment cost and labor cost during the manufacturing.

2.9.2. OpEX. OpEX calculated includes raw material cost, annual operating labor cost, electricity cost, and additional costs which comprises depreciation:

$$\text{OpEX} = C_R + C_{\text{LO}} + C_{\text{EL}} + C_A. \tag{30}$$

C_R, C_{LO}, C_{EL}, and C_A are, respectively, the cost of raw material, the annual operating labor cost, the electricity cost, and the additional cost.

2.9.3. Approximate Profitability Measures. The approximate profitability measures were based on parameters like the annual net cash flow, the payback period, and the return on investment and were computed as explained below.

(1) Net Cash Flow. Net cash flow is actually the difference between total sales and the operating cost

$$\text{Net cash flow} = \text{Total sales} - \text{OpEX}. \tag{31}$$

(2) Payback Period. The payback period (PBP) was computed by dividing the capital cost per the average annual net income.

$$\text{PBP} = \frac{\text{CapEX}}{\text{Annual net income}}. \tag{32}$$

(3) Return on Investment. Return on investment (ROI) was computed by dividing the average annual net income per capital cost.

$$\text{ROI} = \frac{\text{Annual net income}}{\text{CapEX}}. \tag{33}$$

2.9.4. Rigorous Profitability Measure. The rigorous profitability measure calculated was based on the net present, which was calculated as shown below.

(1) Net Present Value. The net present value (NPV) was calculated using [1]

$$\text{NPV} = \sum_1^n \frac{\text{Net cash flow}}{(1+i)^n} - \text{CapEX}. \tag{34}$$

n is the number of years for operating the dryers, and i is the discounting or depreciation rate.

3. Results and Discussion

3.1. Performance Analysis. The performance was assessed by drying 500 g of Cavendish banana with an initial moisture content of 74.4% (wet basis), using the three drying modes, in order to have an idea on the performance of the whole dryer. For all the three modes, the drying process was ended when the final moisture content reached 9.6%. This section
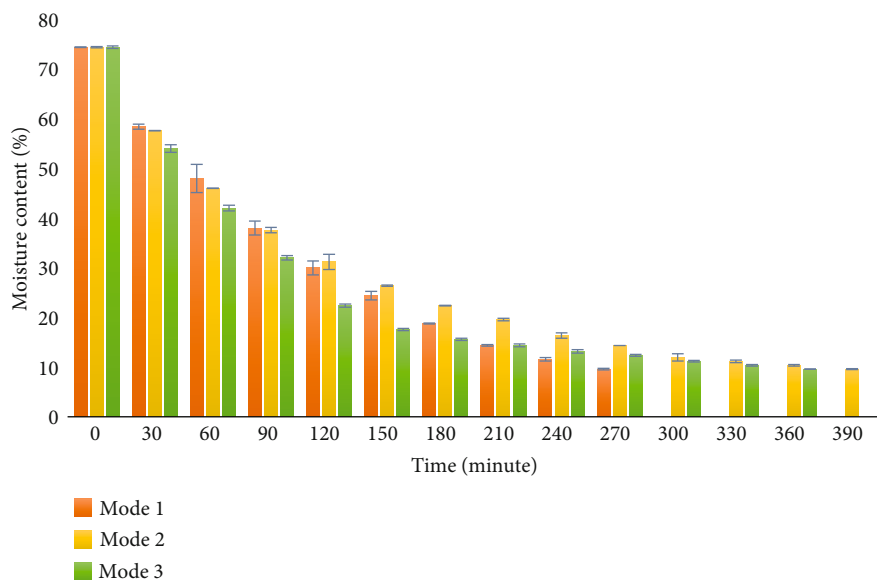
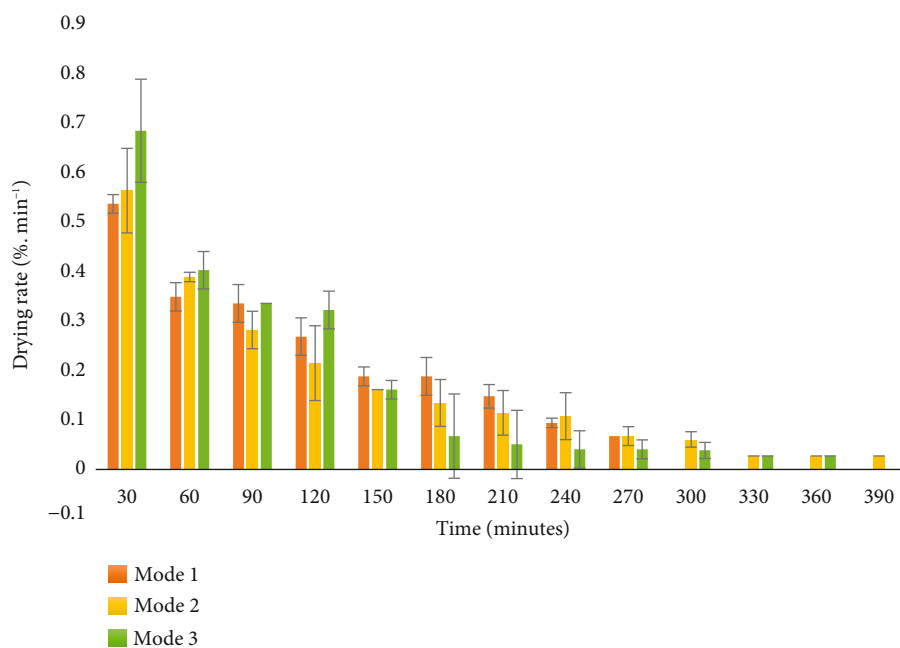FIGURE 2: Moisture content vs time.

FIGURE 3: Drying rate vs time.

discusses various aspects such as the variation of the drying temperature, relative humidity, moisture content, drying rate, specific moisture extraction rate, coefficient of performance, and dryer efficiency to examine the performance of the dryer.

Figures 2–9 show the variation of all the examined parameters as a function of time. In the graphs, the means and standard deviations are presented. As shown in Figure 2, the final moisture content of 9.6% (wet basis) obtained when drying 500 g of Cavendish banana using SAHPD with TES during daytime (mode 1), SAHPD with-

out TES during nighttime (mode 2), and SAHPD without TES during daytime (mode 3) was obtained after the drying time of 270, 390, and 360 minutes, respectively. Thus, the efficiency of the three modes in reducing moisture content is significant. The superior performance of mode 1 becomes evident when compared to modes 2 and 3, as indicated by its significantly reduced drying time of 270 minutes. In contrast to the projections made by Kuan et al. based on the simulation of banana drying using SAHPD, the drying times achieved in this study using modes 1, 2, and 3 are 3.2, 3.5, and 5.25 times shorter, respectively. Additionally, the final
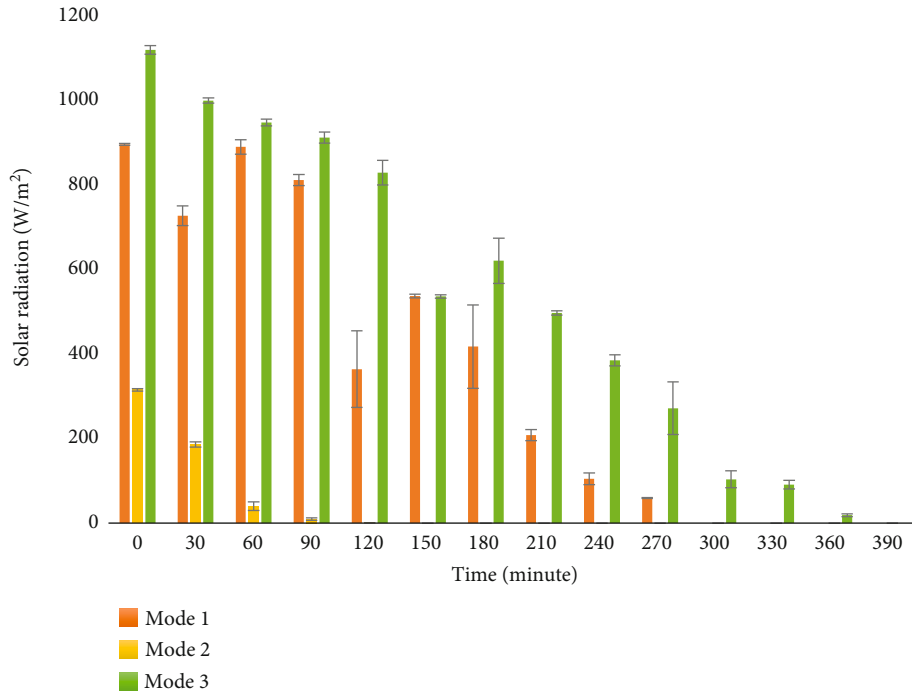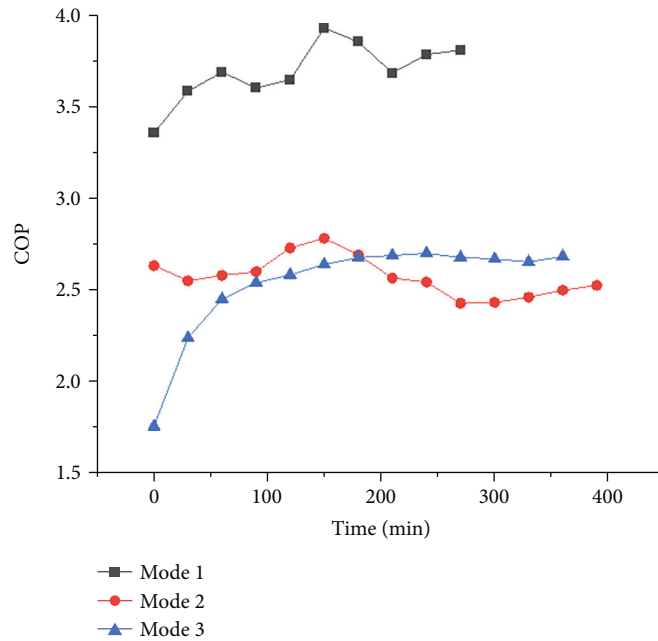
Figure 4: Solar radiation.

Figure 5: Variation of COP during the drying process.

moisture content obtained in this study is half as high as that projected by Kuan et al. [42]. These compelling results serve as a testament to the exceptional efficiency demonstrated by the developed SAHPD across its various operational modes. The average drying temperature and humidity in the drying chamber are the main factors that are observed to have an impact on the reduction of moisture content during the dry-

ing process as depicted in Figure 2. The dryer's inlet temperature rises with time, causing the drying rate to grow initially until it reaches a maximum value; after that, moisture loss from the product causes the drying rate to start decreasing as shown in Figure 3.

The average drying rates achieved in this study using modes 1, 2, and 3 for drying 500 g of Cavendish banana were
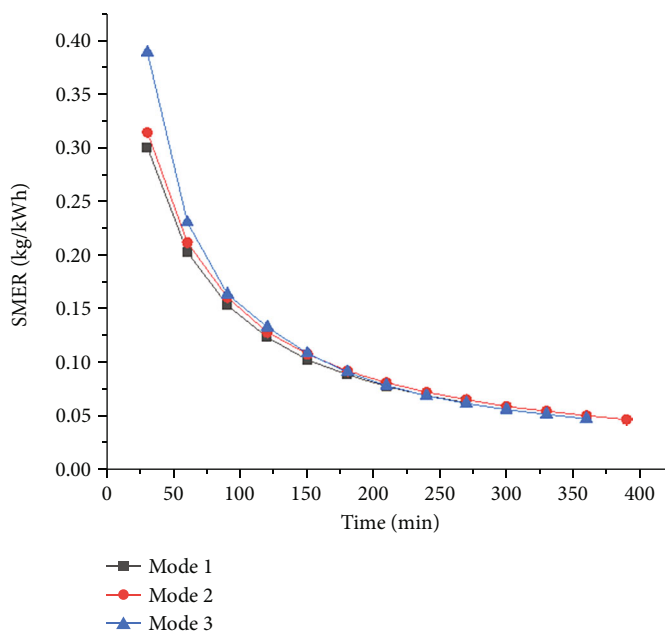
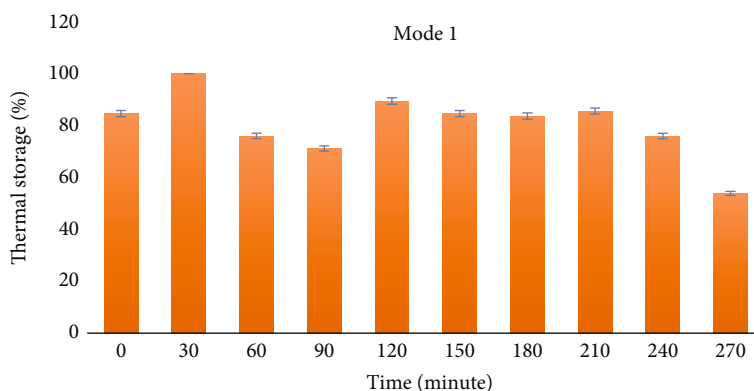FIGURE 6: Variation of SMER vs time.

FIGURE 7: Thermal storage efficiency vs time.

0.24%, 0.16%, and 0.18% per minute, respectively. These findings indicate promising and favorable outcomes when compared to previous studies that have investigated similar drying methods. The results not only validate the effectiveness of the current research but also highlight the potential of the implemented modes to enhance the drying process for Cavendish banana [16]. Figure 4 depicts the variation in solar radiation. This figure shows that unlike modes 1 and 2, when mode 3 was used for drying, the solar radiation disappeared completely after the first hour of drying. This clearly indicates that while using mode 3, the drying process started at the end of the day after sunset and continued into the night in the absence of the sun. This can attest to the high temperatures obtained in the drying chamber when modes 1 and 2 were used. Figure 5 shows how the coefficient of performance (COP) varies with drying time. The average coefficient of performance (COP) values obtained for drying 500 g of Cavendish banana were 3.69, 2.57, and 2.54 for

mode 1, mode 2, and mode 3, respectively. These results underscore the energy-efficient operation and commendable performance of the dryer across the three tested modes. Notably, the maximum COP was achieved when utilizing the solar-assisted heat pump dryer (SAHPD) with thermal energy storage (TES) during daytime, specifically in mode 1. This outcome can be attributed to the reduced energy requirements resulting from the shorter drying time required for 500 g of Cavendish banana. These findings highlight the considerable potential for energy savings and the favorable performance of the SAHPD system, particularly in mode 1. The optimization of energy utilization in this mode contributes to overall operational efficiency, emphasizing the system's capability to deliver efficient and sustainable drying outcomes. The results of COP in modes 1 and 2 are almost identical to those predicted by Kuan et al. [42] when drying banana using SAHPD without thermal energy storage. As a result, the relevance of including
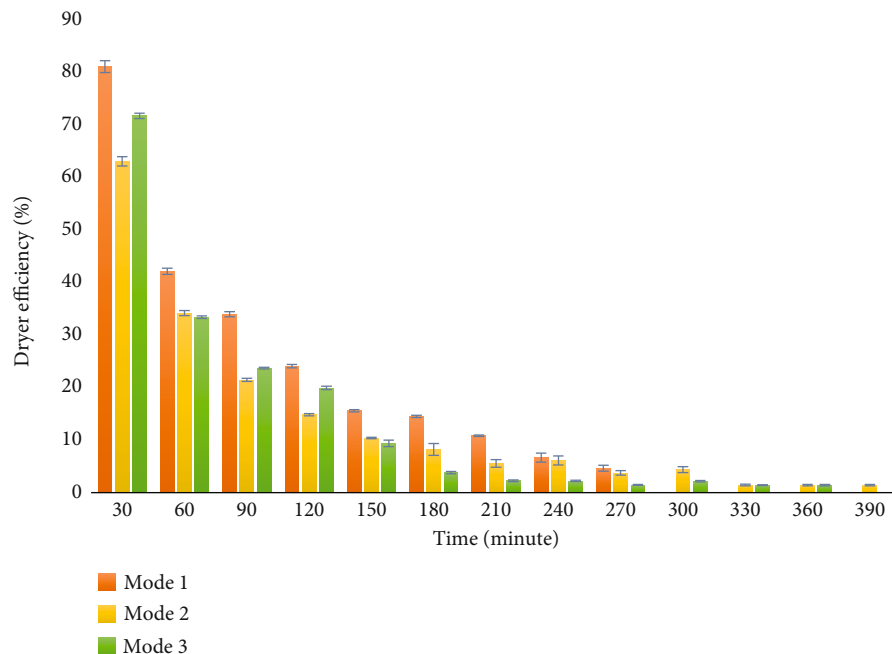
FIGURE 8: Dryer efficiency vs time.

storage in the present dryer can be observed in the high COP attained in mode 1 as opposed to modes 2 and 3. The COP values obtained are acceptable when compared with previous investigations for the drying of bananas using SAHPD [4, 16].

Figure 6 represents the specific moisture extraction rate's variation. This graph shows that, due to a decrease in moisture content, the specific moisture extraction rate dropped quickly with drying time. The average specific moisture extraction rate for 500 g of Cavendish bananas dried in modes 1, 2, and 3 was 0.13 kg/kWh, 0.11 kg/kWh, and 0.12 kg/kWh, respectively; this little difference or variation is attributable to their respective energy consumptions of 5.67, 7.52, and 7.43 kWh. The data obtained during the drying process of Cavendish banana using mode 1 and mode 2 were also used to evaluate the thermal efficiency of the solar collector integrated with thermal storage material (soapstone). Figure 7 describes the variation of thermal efficiency of the solar collector over time when using mode 1. Results showed that the thermal efficiency of the solar collector had the average efficiency of 80.48%. Furthermore, the experimental data were used to calculate drying efficiency which indicates how effectively the drying air removes moisture from the product in the drying chamber. The results for drying efficiency are shown in Figure 8; mode 1 had a higher drying efficiency than modes 2 and 3 due to the average inlet temperature and humidity being higher and lower for mode 1 as compared to other modes. Figure 9 illustrates changes in ambient temperature and relative humidity, as well as temperature and relative humidity at the inlet and outlet of the drying chamber, during the drying of 500 g of Cavendish banana using the three modes. The upper part of this figure displays results for all temperatures, while the lower part displays results for all relative humidities. While drying 500 g of Cavendish banana using mode 1, mode 2, and mode 3, the

results showed that the average ambient temperature was 30.22°C, 26.21°C, and 29.17°C, respectively, and the average relative ambient humidity was 37.39°C, 39.10°C, and 44.43%, respectively. The drying chamber's inlet temperature using modes 1, 2, and 3 was, respectively, 54.17°C, 48.03°C, and 50.63°C. The drying chamber's outlet temperature was, respectively, 48.71°C, 38.40°C, and 47.11°C. The average relative humidity for the three modes at the drying chamber's inlet was 14.83, 14.67, and 18.33%, while it was 17.21, 22.07, and 20.58% at the drying chamber's outlet, for modes 1, 2 and 3, respectively. These findings demonstrate that air enters the drying chamber at a high temperature with low relative humidity and exits at a low temperature with high relative humidity. It can be concluded that when more moisture is extracted from the banana, the temperature drops. The relative humidity of the air rises as a result of the air passing through the drying chamber absorbing moisture from the banana samples.

Although all three tested modes yielded positive results, it was observed that mode 1, which involved the solar-assisted heat pump dryer (SAHPD) with thermal energy storage (TES) during daytime, exhibited the highest temperature and lowest humidity levels in the drying chamber. As a result, this mode achieved shorter drying times and higher coefficients of performance (COP). These findings highlight the crucial role of incorporating TES in the drying process and indicate that solar irradiance variations directly impact temperature fluctuations within the drying chamber. A summary of experimental results obtained from previous references on Cavendish banana drying is presented in Table 1. Notably, these studies often lack comprehensive performance data, as key parameters such as dryer efficiency, drying rate, and specific moisture extraction rate were inconsistently reported. This underscores the need for further research on the drying of Cavendish banana using heat
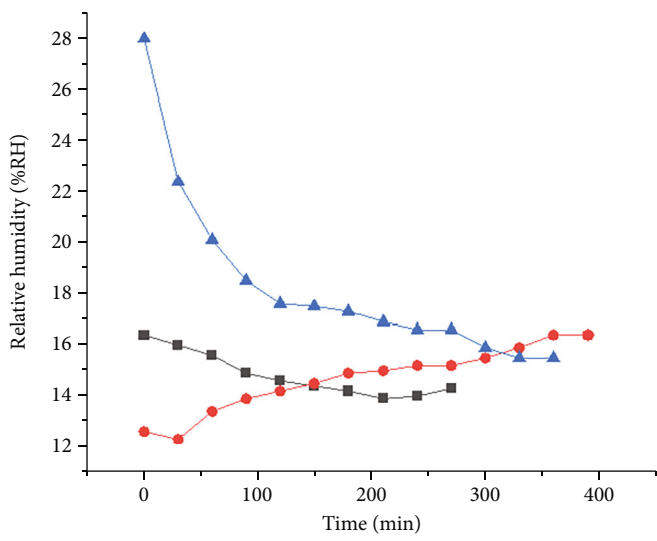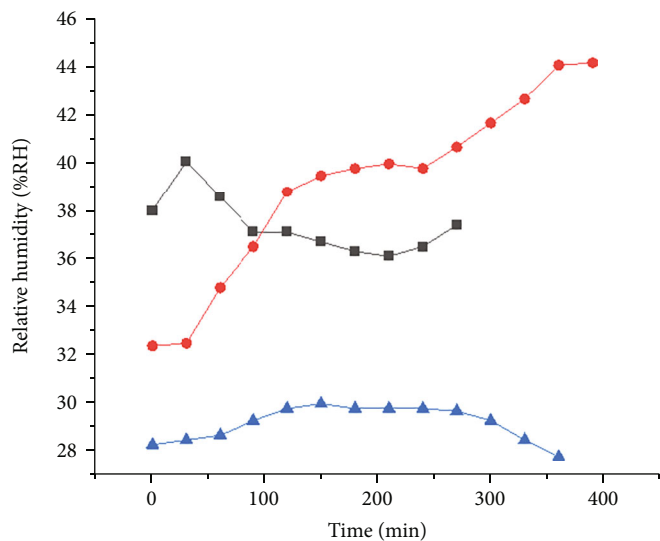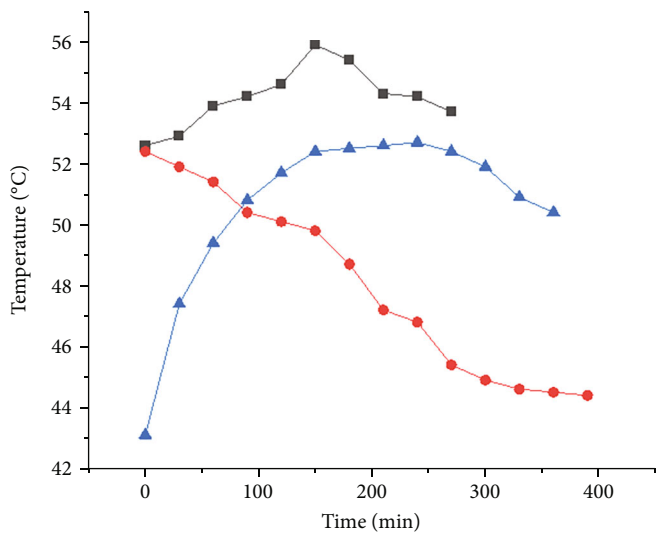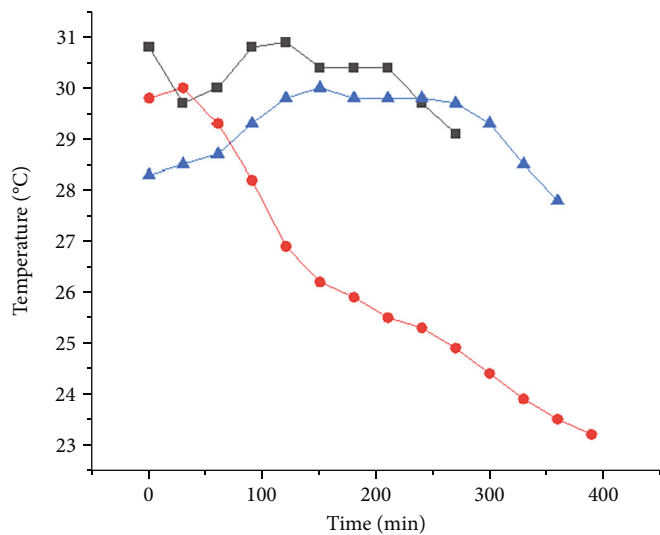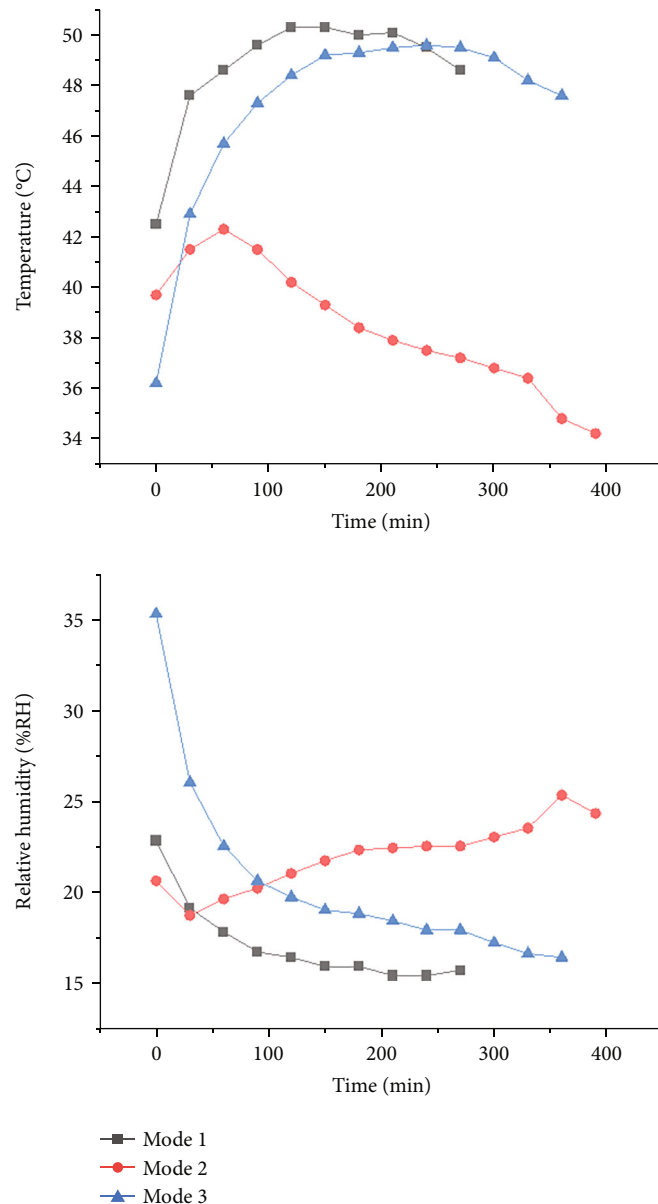
(a)

(b)

Figure 9: Continued.

(c)

Figure 9: Variation of temperature and relative humidity (ambient air (a), inlet (b), and outlet (c) of the drying chamber).

pump dryers. In conclusion, the developed dryer in this study successfully achieved a significantly low final moisture content and demonstrated more favorable drying times compared to previously reported studies. Moreover, the temperatures attained using the developed dryer align with satisfactory levels, as indicated in Table 1. These findings underscore the importance of conducting additional research in the field of Cavendish banana drying, given the limited number of studies exploring the utilization of heat pump dryers for this specific application.

3.2. Proximate, Mineral, and Vitamin Results. The nutritional content of Cavendish banana was evaluated using proximate, mineral, and vitamin analyses before and after drying in the three operating modes. In the graphs, the means

and standard deviations are presented. The results obtained from the proximate parameter analysis, encompassing crude fat, crude ash, crude protein, crude fiber, crude carbohydrates, and moisture are presented in Figure 10. Calorific value outcomes are displayed in Figure 11, while Figure 12 exhibits the results of the mineral parameter analysis, specifically copper, iron, calcium, manganese, phosphorus, and zinc. Additionally, Figure 13 showcases the concentrations of vitamin B6 and vitamin C. Importantly, it is worth noting that the levels of the proximate parameters in the dried Cavendish banana, namely, crude fat, crude ash, crude protein, crude fiber, crude carbohydrates, and moisture, demonstrated statistically insignificant variations ($p > 0.05$) among the three modes that were tested. This suggests that the different operational modes employed during the drying
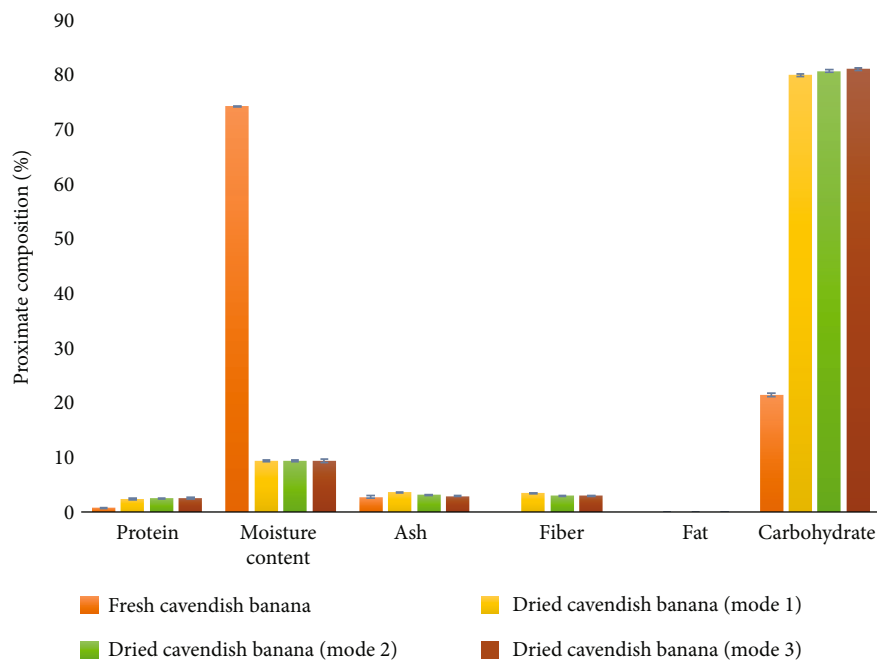
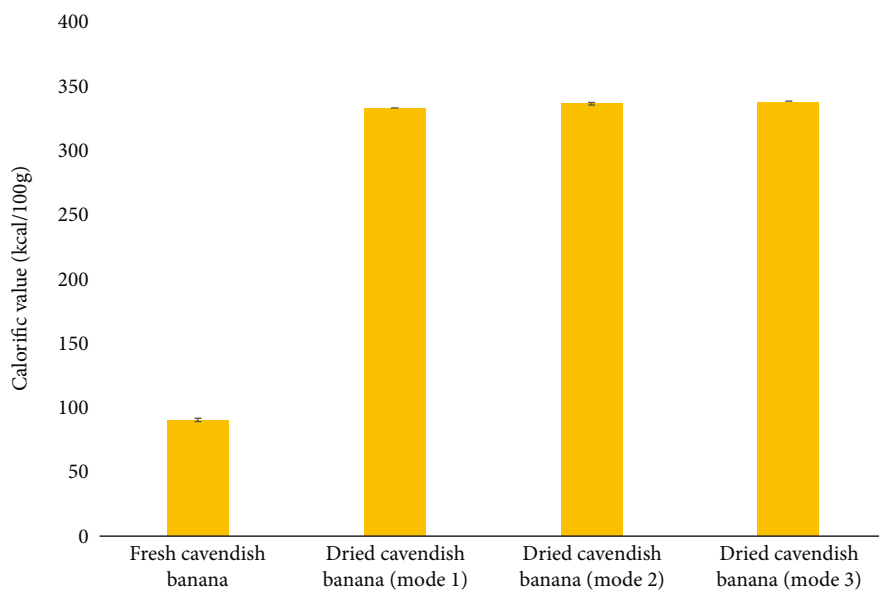FIGURE 10: Proximate composition of Cavendish banana.

FIGURE 11: Calorific value of Cavendish banana.

process had no significant impact on the proximate composition of the dried Cavendish banana. These findings imply that the selected drying modes did not introduce substantial alterations to the nutritional composition of the banana samples. The observed lack of significant variations instills confidence in the consistent and stable nature of the drying process, regardless of the specific operational modes utilized. The dried banana had a significant ($p < 0.05$) concentration of proximate parameters than the fresh Cavendish banana. The findings revealed that carbohydrates, which are the main energy source in the human body [43] were shown to have

the highest proportion of all nutrients evaluated in dried Cavendish banana, with values of 80.1, 80.8, and 81.1% for modes 1, 2, and 3, respectively, compared to fresh Cavendish banana (21.6%). Due to water evaporation, the moisture content of dried Cavendish banana was lower than that of fresh Cavendish banana. The final moisture content value was 9.6% for all the three modes. The moisture content of food products indicates its freshness and shelf life. Foods having a higher moisture content are more sensitive to microbial harm and have a shorter shelf life, which can lead to decomposition [44]. In comparison to fresh Cavendish banana
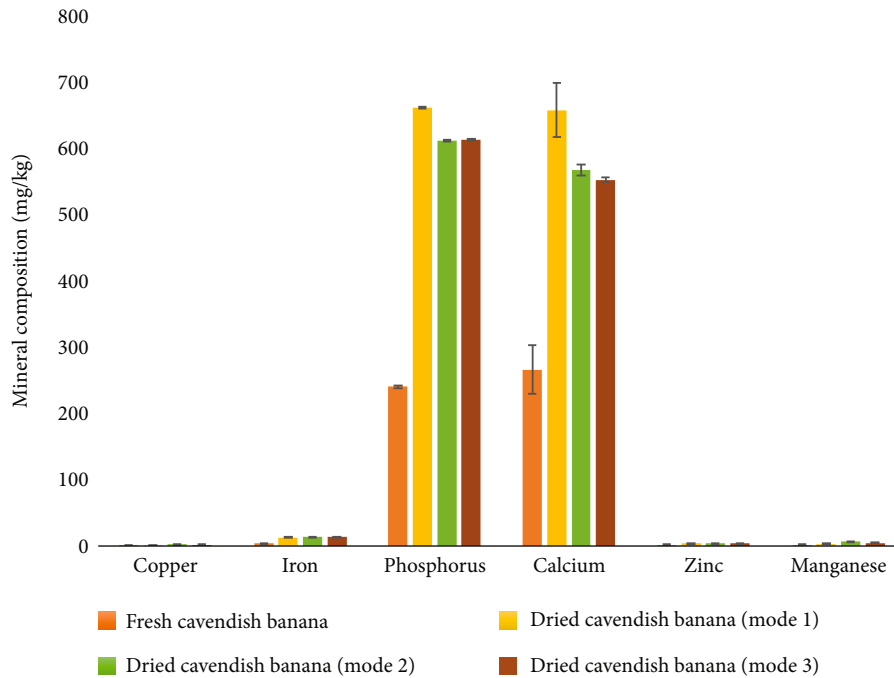
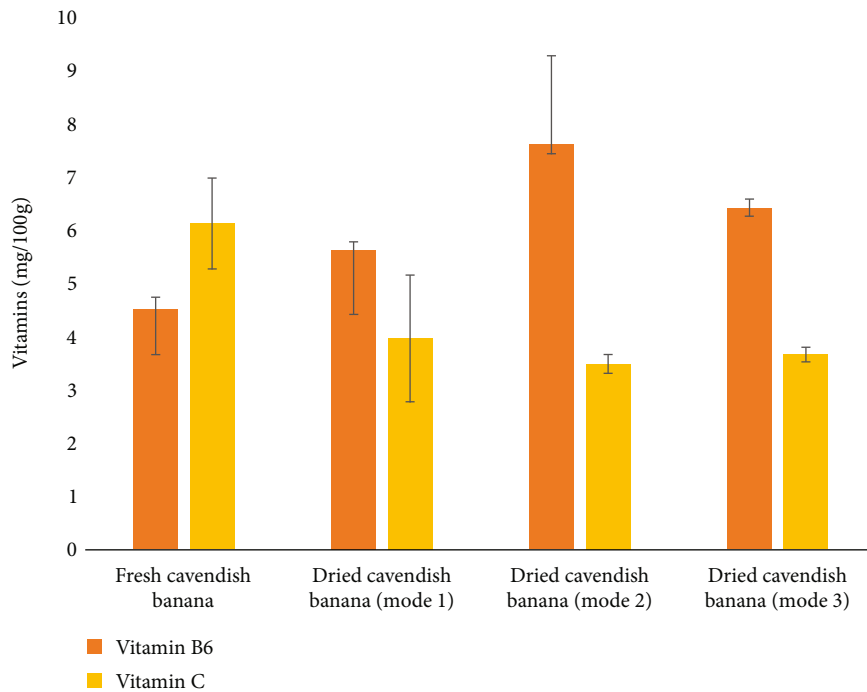Figure 12: Mineral composition of Cavendish banana.

Figure 13: Composition in vitamins B6 and C of Cavendish banana.

(0.008%), the dried Cavendish banana had a greater fat content with values of 0.201, 0.174, and 0.208% using modes 1, 2, and 3, respectively, as shown in Figure 10. Fats are rich in fat-soluble vitamins [44]. The findings also indicate that dried Cavendish banana had a higher protein content than fresh Cavendish banana, with average values of 2.604, 2.782, and

2.704% using mode 1, mode 2, and mode 3, respectively, confirming that moisture loss of dried banana improved nutrient density. Proteins, according to numerous studies, serve a variety of structural and functional roles in the human body. Sufficient protein intake maintains the proper development and functioning of the body [43]. In comparison to the fresh

Cavendish banana (0.048%), the crude fiber was also found to be considerable after drying with values of 3.738, 3.297, and 3.218% using, respectively, mode 1, mode 2, and mode 3. In terms of nutrition, fiber is important. It has been linked to greater elimination of potential mutagens, as well as blood sugar regulation, intestinal health maintenance, and cholesterol reduction [44]. The ash content of dried Cavendish banana increased with values of 3.8, 3.36, and 3.15% using modes 1, 2, and 3, respectively, when compared to fresh Cavendish banana (2.95). This rise could be attributable to moisture loss, which tends to increase nutritional concentration. These ash content values show that the dried Cavendish banana has a good concentration of minerals [44]. The energy value of the dried banana likewise increased significantly when compared to the fresh Cavendish banana (90.2 kcal/100 g), with values of 332.5, 335.9, and 337.1 kcal/100 g using modes 1, 2, and 3, respectively. The obtained results align with those reported by Carughi [45], indicating that fresh Cavendish banana is rich in protein (1.09 g), ash (0.82 g), fiber (2.6 g), fat (0.33 g), carbohydrate (22.84 g), and calorie value (89 kcal). Upon drying, there was a notable increase in the amounts of protein (2.30 g), ash (1.4 g), fiber (7.7 g), fat (33.60 g), carbohydrate (58.40 g), and energy value (519 kcal). These findings indicate that the drying process led to an enhancement in the nutritional content of the Cavendish banana, with elevated levels of key components. Additionally, the results revealed a significant ($p < 0.05$) increase in the concentration of minerals in the dried Cavendish banana compared to its fresh counterpart. This indicates that the drying process contributed to the concentration of minerals, suggesting that the dried Cavendish banana may serve as a more nutrient-dense option compared to its fresh form. The increased protein, ash, fiber, fat, carbohydrate, energy value, and mineral concentration in the dried samples highlight the potential health benefits associated with consuming dried Cavendish banana. These findings provide valuable insights into the nutritional changes that occur during the drying of Cavendish banana. They contribute to the existing knowledge on the nutritional composition of Cavendish banana and emphasize the importance of considering the impact of drying methods on its nutritional profile. Understanding these changes is essential for optimizing the nutritional value and health benefits of dried Cavendish banana, promoting its consumption as a nutritious and convenient snack option.

Minerals are essential parts of our diet. They perform a wide range of tasks, including serving as our bones' building blocks, affecting muscle and nerve activity, and balancing the body's water levels [46, 47]. The results showed that both fresh and dried Cavendish banana contain a considerable portion of calcium and phosphorus. Copper and zinc were found to be present in low amounts among all the minerals analyzed. The concentration of vitamin B6, which is necessary for the growth of the immune system and the brain, increased as a result of all the three modes. Moreover, vitamin B6 promotes metabolism. The three tested modes of drying resulted in significant reductions ($p < 0.05$) in vitamin C concentrations, which can be attributed to the heat sensitivity of this particular vitamin. Similar findings were

TABLE 3: CapEX (capital costs).

Indicators	Value ($)
Cost of materials for manufacturing	2142.88
Cost of insulation materials	47.24
Labor charge for manufacturing	257.29
Purchase cost of the heat pump system	3859.14
Purchase cost of the wiring equipment	99.49
Labor charge for installing the heat pump system	257.29
Purchase cost of the refrigerant	126.5
Total	4647

TABLE 4: OpEX (operating cost).

Indicators	Value ($)
Annual cost of fresh banana	8400
Annual cost of electricity	415.8
Annual labor charge	2400
Depreciation	464.695
Total	11680.5

reported by Carughi [45], who also noted high levels of minerals in fresh Cavendish banana, including calcium (5 mg), copper (0.08 mg), iron (0.26 mg), magnesium (27 mg), manganese (0.27 mg), phosphorus (22 mg), and zinc (0.15 mg). Following the drying process, the concentrations of calcium (18 mg), copper (0.21 mg), iron (1.25 mg), magnesium (76 mg), manganese (1.56 mg), phosphorus (56 mg), and zinc (0.75 mg) all increased. Moreover, Carughi demonstrated that fresh Cavendish banana contains vitamin C (8.7 mg); however, the drying process led to a reduction in vitamin C concentration, resulting in a value of 6.3 mg. These findings emphasize the impact of drying on the nutritional composition of Cavendish banana, particularly the heat sensitivity of vitamin C. Despite the reduction in vitamin C levels, the dried Cavendish banana exhibited increased mineral concentrations, including essential elements such as calcium, copper, iron, magnesium, manganese, phosphorus, and zinc. These changes indicate that while there may be some nutrient loss during the drying process, the dried Cavendish banana retains valuable minerals that contribute to its nutritional value.

3.3. Economic Analysis. The economic feasibility of the SAHPD with TES was assessed using mode 1 based on CapEX (capital costs), OpEX (operating costs), and approximate profitability measures based on indicators such as the annual net cash flow, the payback period, and the return on investment, as well as rigorous profitability measure with the net present value as an indicator. The economic analysis was based on the economic conditions in Tanzania in 2023. Tables 3–7 summarize the results of all parameters calculated and assumptions made for the economic analysis of drying Cavendish banana. As shown in Table 3, CapEX was calculated by including the equipment costs and the labor cost during the manufacturing. OpEX was calculated by including the annual cost of fresh banana, annual cost

Table 5: Annual sale estimation.

Indicators	Value ($)
Price of 1 kg of the dried banana	3.5
Total banana dried per year	4200
Annual sales of the dried banana	14700

Table 6: Approximate profitability measures.

Indicators	Value
Net cash flow	$3019.5
Payback period	1.5 years
Return on investment	65%

Table 7: Rigorous profitability measure (calculation of NPV).

Year	Net cash flow	10% discount rate	Present value	Unit
1	3019.505	0.90909091	2745.004545	
2	3019.505	0.82644628	2495.458678	
3	3019.505	0.7513148	2268.598798	
4	3019.505	0.68301346	2062.362544	
5	3019.505	0.62092132	1874.87504	
6	3019.505	0.56447393	1704.431854	
7	3019.505	0.51315812	1549.483504	
8	3019.505	0.46650738	1408.621367	
9	3019.505	0.42409762	1280.564879	
10	3019.505	0.38554329	1164.14989	
Cumulative present value			18553.5511	$
Net present value (NPV)			13906.6	$

of electricity, annual operating labor charge, and the depreciation as shown in Table 4. CapEX and OpEX were determined to be $4647 and $11680.5, respectively. These values of CapEX and OpEX indicate the costs necessary for manufacturing the developed dryer and generate income, respectively. As shown in Table 5, according to the estimation, by using SAHPD with TES (mode 1), 4200 kg of dried banana may be produced annually for 300 working days and sold for $3.5/kg. This results in an expected annual cash flow of $3019.5 as indicated in Table 6. This income is very reasonable when compared to the OpEX. Results in Table 6 also showed that the payback period is 1.5 years. It means that the cash flows will therefore be able to absorb the cost generated by the investment after 1.5 years. In Table 6, the return on investment is determined to be 65%. This significant return on investment indicates that the developed dryer is profitable and poses little investment risk. The net present value is $13906.6 as indicated in Table 7. This result confirms in addition to the payback and the return on investment that the developed dryer is profitable because an investment with a higher net present value is considered to be more attractive. The developed SAHPD with TES is therefore an economically viable option for drying banana.

4. Conclusion

This research investigated a novel solar-assisted heat pump dryer integrated with thermal energy storage using three different operating modes: mode 1 (daytime with thermal energy storage), mode 2 (nighttime without thermal energy storage), and mode 3 (daytime without thermal energy storage). Drying experiments using 500 g of Cavendish banana were conducted, and the study included an economic and performance analysis of the dryer, as well as proximate, mineral, and vitamin analyses of the fresh and dried Cavendish banana. The results demonstrated a significant reduction in moisture content from 74.4% to 9.6% after drying for 270, 390, and 360 minutes in modes 1, 2, and 3, respectively. The drying rates ranged from 0.16% to 0.24% per minute, indicating the efficiency of the dryer in removing moisture. The average specific moisture extraction rate varied between 0.11 kg/kWh and 0.13 kg/kWh across the three modes, highlighting the effectiveness of energy utilization. Furthermore, the coefficient of performance for the dryer was determined to be 3.69, 2.57, and 2.54 for modes 1, 2, and 3, respectively, illustrating their energy efficiency in different operating conditions. The economic analysis revealed favorable economic indicators, with a payback period of 1.5 years and a return on investment of 65%. This suggests that the investment in the developed dryer can be recovered within a relatively short time frame. The results showed that both fresh and dried Cavendish bananas contain a considerable portion of calcium and phosphorus. Copper and zinc were found to be present in low amounts. The concentration of vitamin B6 increased as a result of all three modes. However, due to its heat sensitivity, concentrations of vitamin C decreased after drying. The findings emphasize the significance of integrating the thermal energy storage system with soapstone to enhance the performance and efficiency of the solar-assisted heat pump dryer in agricultural product drying. Future research directions should explore alternative storage materials and refrigerants to optimize the dryer's operation. Additionally, attention should be given to the configuration and design of the energy storage system to further improve its effectiveness and overall performance in drying applications. By addressing these areas, the solar-assisted heat pump dryer can be further optimized and contribute to sustainable and efficient drying processes in the agricultural sector.

Abbreviations

SAHPD: Solar-assisted heat pump dryer
W: Watt
kW: Kilowatt
kWh: Kilowatt-hour
COP: Coefficient of performance
S: Surface
MC: Moisture content
H: Hour
I: Initial
F: Final
T_{in}: Drying chamber's inlet temperature

T_{out}:	Drying chamber's outlet temperature
T_a:	Temperature of the ambient air
V:	Velocity
M_w:	Mass of water removed
RH_{in}:	Relative humidity at the drying chamber's inlet
RH_{out}:	Relative humidity at the drying chamber's outlet
DR:	Drying rate
TES:	Thermal energy storage
°C:	Degree Celsius
%:	Percentage
db:	Dry basis
wb:	Wet basis
m:	Meter
s:	Second
min:	Minute
ρ:	Density
Cond:	Condenser
$\dot{m}$:	Mass flow rate
kJ:	Kilojoule
C_p:	Specific heat
$:	American dollars
Q:	Heating capacity
t:	Time
RH_a:	Relative humidity of the ambient air
kg:	Kilogram.

Data Availability

The data supporting the findings of the study are available and will be provided upon reasonable request by the corresponding author.

Conflicts of Interest

All authors declare that they have no conflicts of interest.

Acknowledgments

References

[1] S. Mohammed, N. Fatumah, and N. Shadia, "Drying performance and economic analysis of novel hybrid passive-mode and active-mode solar dryers for drying fruits in East Africa," *Journal of Stored Products Research*, vol. 88, article 101634, 2020.

[2] M. U. Hasan, A. U. Malik, S. Ali et al., "Modern drying techniques in fruits and vegetables to overcome postharvest losses: a review," *Journal of Food Processing and Preservation*, vol. 43, no. 12, Article ID e14280, 2019.

[3] M. Mohanraj, Y. Belyayev, S. Jayaraj, and A. Kaltayev, "Research and developments on solar assisted compression heat pump systems – a comprehensive review (part-B: applications)," *Renewable and Sustainable Energy Reviews*, vol. 83, pp. 124–155, 2018.

[4] A. Loemba, B. Kichonge, and T. Kivevele, "Comprehensive assessment of heat pump dryers for drying agricultural products," *Energy Science & Engineering*, vol. 11, no. 8, pp. 2985–3014, 2023.

[5] Y. Wang, M. Li, Y. Qiu et al., "Performance analysis of a secondary heat recovery solar-assisted heat pump drying system for mango," *Energy Exploration & Exploitation*, vol. 37, no. 4, pp. 1377–1387, 2019.

[6] M. Yu and J. Yu, "Thermodynamic analyses of a solar assisted ejector enhanced vapor injection cycle with subcooler for heat pump dryer application," *Solar Energy*, vol. 232, pp. 376–387, 2022.

[7] A. Badiei, Y. G. Akhlaghi, X. Zhao et al., "A chronological review of advances in solar assisted heat pump technology in 21st century," *Renewable and Sustainable Energy Reviews*, vol. 132, article 110132, 2020.

[8] M. Yahya, H. Fahmi, A. Fudholi, and K. Sopian, "Performance and economic analyses on solar-assisted heat pump fluidised bed dryer integrated with biomass furnace for rice drying," *Solar Energy*, vol. 174, pp. 1058–1067, 2018.

[9] A. Alishah, M. V. Kiamahalleh, F. Yousefi, A. Emami, and M. V. Kiamahalleh, "Solar-assisted heat pump drying of coriander: an experimental investigation," *International Journal of Air-Conditioning and Refrigeration*, vol. 26, no. 4, article 1850037, 2018.

[10] N. S. Prasanna and B. Manjula, "Review on drying of agricultural produce using solar assisted heat pump drying," *International Journal of Agricultural Engineering*, vol. 11, no. 2, pp. 409–420, 2018.

[11] A. Singh, J. Sarkar, and R. R. Sahoo, "Experimental performance analysis of novel indirect-expansion solar-infrared assisted heat pump dryer for agricultural products," *Solar Energy*, vol. 206, pp. 907–917, 2020.

[12] A. Singh, J. Sarkar, and R. R. Sahoo, "Experimental energy, exergy, economic and exergoeconomic analyses of batch-type solar-assisted heat pump dryer," *Renewable Energy*, vol. 156, pp. 1107–1116, 2020.

[13] A. B. T. Loemba, B. Kichonge, J. R. Selemani, and T. Kivevele, "Performance evaluation of solar-assisted heat pump dryer integrated with thermal energy storage for drying Moringa oleifera leaves," *MRS Advances*, vol. 8, no. 12, pp. 698–702, 2023.

[14] M. Mohanraj, Y. Belyayev, S. Jayaraj, and A. Kaltayev, "Research and developments on solar assisted compression heat pump systems – a comprehensive review (part a: modeling and modifications)," *Renewable and Sustainable Energy Reviews*, vol. 83, pp. 90–123, 2018.

[15] M. Yahya, H. Fahmi, R. Hasibuan, and A. Fudholi, "Development of hybrid solar-assisted heat pump dryer for drying paddy," *Case Studies in Thermal Engineering*, vol. 45, article 102936, 2023.

[16] A. Singh, J. Sarkar, and R. R. Sahoo, "Experimentation on solar-assisted heat pump dryer: thermodynamic, economic and exergoeconomic assessments," *Solar Energy*, vol. 208, pp. 150–159, 2020.

[17] M. C. Pinheiro, R. Madaleno, and L. M. Castro, "Drying kinetics of two fruits Portuguese cultivars (Bravo de Esmolfe apple and Madeira banana): an experimental study," *Heliyon*, vol. 8, no. 4, article e09341, 2022.

[18] T. H. Ferreira and M. L. Freitas, "Production, physical, chemical and sensory evaluation of dried banana (Musa Cavendish)," *Emirates Journal of Food and Agriculture*, vol. 31, pp. 102–108, 2019.

[19] R. C. P. Braga, S. P. Ruiz, and D. S. de Aquino, "Drying kinetics and the effect of blanching pretreatment on banana," *Revista Brasileira de Tecnologia Agroindustrial*, vol. 15, no. 2, 2021.

[20] Y. Gu, L. Zhen, and H. Jiang, "Mathematical analysis of temperature distribution uniformity of banana dried by vacuum radio frequency treatment," *Drying Technology*, vol. 38, no. 15, pp. 2027–2038, 2020.

[21] V. Nguyen, H. Tran, and T. Phan, "Effect of pre-treatments on qualities and storage life of banana dried by using solar dryer dome," *IOP Conference Series: Earth and Environmental Science*, vol. 1155, no. 1, article 012020, 2023.

[22] R. Dandamrongrak, R. Mason, and G. Young, "The effect of pretreatments on the drying rate and quality of dried bananas," *International Journal of Food Science & Technology*, vol. 38, no. 8, pp. 877–882, 2003.

[23] M. Abubakar and D. Isiyaku, "Development of a par-boiled rice solar dryer," *Bayero Journal of Pure and Applied Sciences*, vol. 7, no. 2, pp. 1–7, 2015.

[24] E.-A. O. M. A. Akoy, M. A. Ismail, E.-F. A. Ahmed, and W. Luecke, "Design and Construction of a Solar Dryer for Mango Slices," in *Proceedings of International Research on Food Security, Natural Resource Management and Rural Development-Tropentag. University of Bonn*, Bonn, Germany, 2006.

[25] A. Fudholi, S. Mat, D. F. Basri, M. H. Ruslan, and K. Sopian, "Performances analysis of greenhouse solar dryer with heat exchanger," *Contemporary Engineering Sciences*, vol. 9, no. 3, pp. 135–144, 2016.

[26] C. A. Komolafe and M. A. Waheed, "Design and fabrication of a forced convection solar dryer integrated with heat storage materials," *Annales de Chimie Science des Matériaux*, vol. 42, no. 1, pp. 22–39, 2018.

[27] N. R. Nwakuba, S. Asoegwu, and K. Nwaigwe, "Energy requirements for drying of sliced agricultural products: a review," *Agricultural Engineering International: CIGR Journal*, vol. 18, no. 2, pp. 144–155, 2016.

[28] H. Chirino, B. Xu, X. Xu, and P. Guo, "Generalized diagrams of energy storage efficiency for latent heat thermal storage system in concentrated solar power plant," *Applied Thermal Engineering*, vol. 129, pp. 1595–1603, 2018.

[29] B. Abu-Jdayil, A.-H. Mourad, W. Hittini, M. Hassan, and S. Hameedi, "Traditional, state-of-the-art and renewable thermal building insulation materials: an overview," *Construction and Building Materials*, vol. 214, pp. 709–735, 2019.

[30] J. M. Singer, A. C. Pedroso-de-Lima, N. I. Tanaka, and V. A. González-López, "To triplicate or not to triplicate?," *Chemometrics and Intelligent Laboratory Systems*, vol. 86, no. 1, pp. 82–85, 2007.

[31] A. U. Sundari and E. Veeramanipriya, "Performance evaluation, morphological properties and drying kinetics of untreated Carica papaya using solar hybrid dryer integrated with heat storage material," *Journal of Energy Storage*, vol. 55, article 105679, 2022.

[32] M. Aktaş, A. Khanlari, A. Amini, and S. Şevik, "Performance analysis of heat pump and infrared–heat pump drying of grated carrot using energy-exergy methodology," *Energy Conversion and Management*, vol. 132, pp. 327–338, 2017.

[33] A. Singh, J. Sarkar, and R. R. Sahoo, "Experimental energy-exergy performance and kinetics analyses of compact dual-mode heat pump drying of food chips," *Journal of Food Process Engineering*, vol. 43, no. 6, article e13404, 2020.

[34] M. Mohanraj, "Performance of a solar-ambient hybrid source heat pump drier for copra drying under hot-humid weather conditions," *Energy for Sustainable Development*, vol. 23, pp. 165–169, 2014.

[35] S. Kesavan, T. V. Arjunan, and S. Vijayan, "Thermodynamic analysis of a triple-pass solar dryer for drying potato slices," *Journal of Thermal Analysis and Calorimetry*, vol. 136, no. 1, pp. 159–171, 2019.

[36] M. A. Izquierdo-Barrientos, C. Sobrino, and J. A. Almendros-Ibáñez, "Thermal energy storage in a fluidized bed of PCM," *Chemical Engineering Journal*, vol. 230, pp. 573–583, 2013.

[37] AOAC, *Official methods of analysis*, Association of official analytical chemist, W. D. C., USA, 19th edition, 2012.

[38] AOAC, "Official Methods of Analysis of The Association of Official Analytical Chemists," in *Vitamin C (ascorbic acid) method 43.051, I & II*, AOAC, 1990.

[39] L. Jorhem, J. Engman, Collaborators: et al., "Determination of lead, cadmium, zinc, copper, and iron in foods by atomic absorption spectrometry after microwave digestion: NMKL1 collaborative study," *Journal of AOAC International*, vol. 83, no. 5, pp. 1189–1203, 2000.

[40] N. P. Bineesh, R. S. Singhal, and A. B. Pandit, "A study on degradation kinetics of ascorbic acid in drumstick (*Moringa oleifera*) leaves during cooking," *Journal of the Science of Food and Agriculture*, vol. 85, no. 11, pp. 1953–1958, 2005.

[41] A. Ogunneye, O. Banjoko, M. Gbadamosi, O. Falegbe, K. Moberuagba, and O. Badejo, "Spectrophotometic determination of caffeine and vitamin B6 in selected beverages, energy/soft drinks and herbal products," *Nigerian Journal of Basic and Applied Sciences*, vol. 28, no. 1, pp. 22–29, 2020.

[42] M. Kuan, Y. Shakir, M. Mohanraj, Y. Belyayev, S. Jayaraj, and A. Kaltayev, "Numerical simulation of a heat pump assisted solar dryer for continental climates," *Renewable Energy*, vol. 143, pp. 214–225, 2019.

[43] M. M. A. N. Ranjha, S. Irfan, M. Nadeem, and S. Mahmood, "A comprehensive review on nutritional value, medicinal uses, and processing of banana," *Food Reviews International*, vol. 38, no. 2, pp. 199–225, 2022.

[44] J. Dotto, A. O. Matemu, and P. A. Ndakidemi, "Nutrient composition and selected physicochemical properties of fifteen Mchare cooking bananas: a study conducted in northern Tanzania," *Scientific African*, vol. 6, article e00150, 2019.

[45] A. Carughi, "Bananas, dried bananas, and banana chips: nutritional characteristics, phytochemicals, and health effects," *Dried Fruits*, pp. 414–427, 2013.

[46] M.-H. Kim and M.-K. Choi, "Seven dietary minerals (Ca, P, Mg, Fe, Zn, Cu, and Mn) and their relationship with blood pressure and blood lipids in healthy adults with self-selected diet," *Biological Trace Element Research*, vol. 153, no. 1-3, pp. 69–75, 2013.

[47] C. Weyh, K. Krüger, P. Peeling, and L. Castell, "The role of minerals in the optimal functioning of the immune system," *Nutrients*, vol. 14, no. 3, p. 644, 2022.